Dedicated to Professor Ioan-Iovitz Popescu's 80th Anniversary

DEFECT LATTICE SOLITONS
IN TWO-DIMENSIONAL KERR MEDIA

HONG WANG[1], WEI HE[1], XING ZHU[2], YINGJI HE[3]

[1] South China University of Technology, Guangdong Engineering Research Center for Solid State
Lighting, School of Science, Guangzhou 510640, China.
[2] State Key Laboratory of Optoelectronic Materials and Technologies, Sun Yat-Sen University,
510275 Guangzhou, China
[3] Guangdong Polytechnic Normal University, School of Electronics and Information,
510665 Guangzhou, China; E-mail: phhwang@scut.edu.cn

Abstract. We report on the existence and stability of two-dimensional fundamental defect solitons in optical lattices based on both focusing and defocusing Kerr media. It is found that in focusing Kerr media, for positive defect, the solitons only exist in the semi-infinite gap; for negative defect, the solitons may stably exist in the semi-infinite and the first gaps. In contrast, in defocusing Kerr media, for positive defect, the solitons exist in both the first gap and semi-infinite gap; while for negative defect, the solitons only exist in the first gap. Additionally, for zero defect, solitons only exist in the semi-infinite gap for focusing media and only exist in the first gap for defocusing media.

Key words: Kerr media, optical lattices, defect solitons.

1. INTRODUCTION

Solitons are localized waves that propagate in nonlinear media where dispersion and diffraction exist. In optics, the existence of solitons in periodic optical lattices with nonlinearity has gotten a lot of attention in the past dacade [1–5]. These solitons were studied both theoretically and experimentally, and some of them were observed by different groups [6–10]. Gap solitons are formed by the nonlinear coupling between forward- and backward-propagating light waves [11–13]. Gap solitons are significant to the fundamental studies in optics and photonics [14, 15].

Defect linear modes [10, 16, 17] and nonlinear modes (solitons) [2, 18–21] have been widely studied in both one-dimensional (1D) and two-dimensional (2D) optical lattices with a single defect. Defect solitons (DSs) have been studied in different types of 2D optical lattices based on focusing saturable nonlinear media, and the obtained results show that these DSs exist in different bandgaps with different defect intensity [18–21].

In this paper, we study the DSs in two-dimensional optical lattices based on both focusing and defocusing Kerr media. In focusing Kerr media, for positive defect and zero defect (uniform lattices), the solitons only exist in the semi-infinite gap and all these solitons are stable. For negative defect, the solitons may stably exist in the semi-infinite and the first gaps. But at the edge of the band, solitons are unstable. In contrast, in defocusing Kerr media, for positive defect, the solitons exist in both the first gap and the semi-infinite gap; while for negative and zero defects, the solitons only exist in the first gap and these solitons are stable. Our results also demonstrate that the stability of DSs in the case of focusing nonlinearity obeys the Vakhitov-Kolokolov (VK) criterion, and the stability of DSs in the case of defocusing nonlinearity obeys the anti-VK criterion [22].

2. THE THEORETICAL MODEL

The optical beam propagating in the Kerr media with optical lattices is described by the following nonlinear Schrödinger equation [22–25]:

$$i\frac{\partial U}{\partial z} + \frac{\partial^2 U}{\partial x^2} + \frac{\partial^2 U}{\partial y^2} + V(x,y)U + \gamma |U|^2 U = 0, \tag{1}$$

where $U(x,y,z)$ is a real function representing the slowly varying amplitude of the probe beam, (x,y) are transverse axis, z is the propagation distance and $\gamma = \pm 1$ (for a focusing medium $\gamma = 1$, whereas for a defocusing one $\gamma = -1$). Here $V(x,y)$ is the periodic lattice potential with a single defect as described by

$$V(x,y) = V_0(\cos^2 x + \cos^2 y)\{1 + \varepsilon \exp[-(x^2+y^2)^4/128]\}, \tag{2}$$

where V_0 is the depth of the optical potential and ε is the defect intensity. When $\varepsilon > 0$, it represents a positive defect, $\varepsilon = 0$ represents a uniform lattice without defect, whereas $\varepsilon < 0$ represents a negative defect. The positive and negative defects are respectively attractive and repulsive as concerned the interaction of solitons with them. In this work, we set $V_0 = 6$ [24, 25]. The intensity distribution of lattice potential with negative defect ($\varepsilon = -0.2$) and positive defect ($\varepsilon = 0.2$) are shown in Figs. 1a and 1b, respectively.

In order to get the bandgap structure, we can write $U(x,y,z)$ as, $U(x,y,z)=u(x,y)\exp[i(k_x x+k_y y)+i\mu z]$, where $u(x,y)$ is a periodic function with the same periodicity of the lattices, μ is the real propagation constant, k_x and k_y are wave numbers in the first Brillouin zone. By substituting it into Eq. 1) and using the plane wave expansion method [26] we can obtain the semi-infinite gap as $\mu > 7.88$, the first gap as $4.78 \leq \mu \leq 7.46$, and the second gap as $2.19 \leq \mu \leq 2.91$. As indicated in Fig. 1c, there are only three gaps in our optical structure.
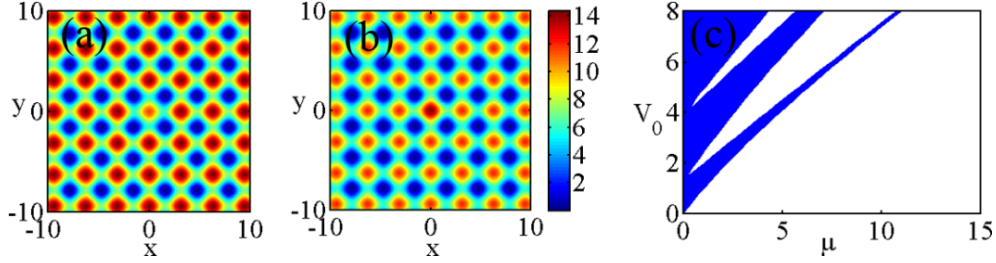
Fig. 1 (Color online) – a) The lattice potential with a negative defect at the center $\varepsilon = -0.2$;
b) $\varepsilon = 0.2$; c) bandgap structure of the optical potential (blue shaded regions are Bloch bands).

The soliton solutions of Eq. (1) are sought in the form of $U(x, y, z) = u(x, y)\exp(i\mu z)$, where $u(x, y)$ is a real-valued function. By substituting this expression to Eq. (1) we get the following equation:

$$\frac{\partial^2 u}{\partial x^2} + \frac{\partial^2 u}{\partial y^2} + Vu + \gamma |u|^2 u = \mu u .\qquad(3)$$

There are several methods to solve this equation; here the modified squared-operator iteration method (MSOM) is used to numerically solve the equation, see Ref. [25].

To study the stability of defect solitons, we perturb them as

$$U(x, y, z) = \{u(x, y) + [v(x, y) - w(x, y)]\exp(\lambda z) + [v(x, y) + w(x, y)]^* \cdot \\ \cdot \exp(\lambda^* z)\}\exp(i\mu z),\qquad(4)$$

where the superscript "*" represents the complex conjugation, and $v, w \ll 1$. Substituting these perturbations into Eq. (1) and linearizing it, we can get the following linear eigenvalue problem

$$L\begin{pmatrix} v \\ w \end{pmatrix} = -i\lambda \begin{pmatrix} v \\ w \end{pmatrix},\qquad(5)$$

where $L = \begin{pmatrix} 0 & L_0 \\ L_1 & 0 \end{pmatrix}$, $L_0 = -(\frac{\partial^2}{\partial x^2} + \frac{\partial^2}{\partial y^2}) - V + \mu - \gamma u^2$, $L_1 = -(\frac{\partial^2}{\partial x^2} + \frac{\partial^2}{\partial y^2}) - V + \mu - 3\gamma u^2$,

and λ is the eigenvalue. The growth rate Re (λ) can be solved by a numerical method called the original operator iteration method (OOM) [27]. If there exists an eigenvalue λ with Re (λ) > 0, the defect solitons are linearly unstable, otherwise, the solitons are linearly stable. The power of solitons defined by $P = \int_{-\infty}^{+\infty} \int_{-\infty}^{+\infty} |u|^2 \, dxdy$ is conserved upon propagation. We also add a white noise (10% of the initial soliton profiles) in order to simulate the propagation of perturbed solitons.

3. NUMERICAL RESULTS

3.1. THE DEFECT SOLITONS IN FOCUSING KERR MEDIA

First, we consider the uniform lattice ($\varepsilon = 0$, i.e., without any defect in the lattice). The solitons only exist in the semi-infinite gap. The soliton power *P versus* the propagation constant μ is plotted in Fig. 2a. As shown in the figure, the power *P* monotonously increases with the growth of μ. In uniform lattices, the solitons are stable in the semi-infinite gap. We numerically solve the Eq. (5), and find that the real part of perturbation growth rate Re (λ) is always zero. As a typical example, we choose $\mu = 10$ [point A in Fig. 2a] to simulate the propagation of the soliton. From Figs. 3a–3c, we can find that the soliton is trapped in one cell of the lattice and can be stable in propagation.
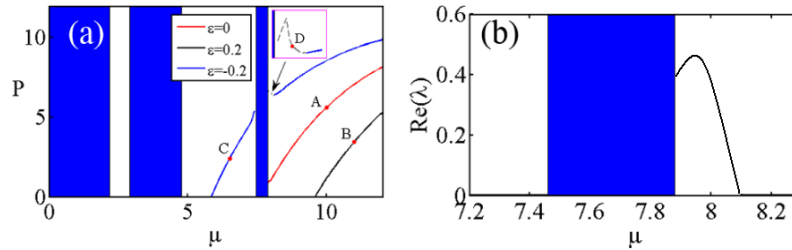

Fig. 2 (Color online) – a) The power of DSs *versus* propagation constant in focusing media
(blue shaded regions are Bloch bands); b) the real part of perturbation growth rate
for the unstable DS when $\varepsilon = -0.2$.

Next, we take $\varepsilon = 0.2$ as a typical positive defect of the lattice in order to study DSs. The DSs' power versus the propagation constant μ is plotted in Fig. 2a. The solitons only exist in the semi-infinite gap, a feature which is similar to that occurring in the case of DSs in the saturated nonlinear media [18]. Compared with the power curve of solitons in uniform lattice, the power of positive DSs is smaller than that in the case of uniform lattice for certain propagation constant. And the DSs in positive defect lattices are stable too. Accordingly, we also get that the real part of perturbation growth rate is zero. Fig. 3d shows the profile of DS for $\mu = 11$ [point B in Fig. 2a], and Figs. 3e and 3f are the profiles of DS at $z = 100$ and $z = 200$, respectively. Apparently, the solitons in the case of positive defects can keep their profiles during propagation. Note that in this case the region of the stable DSs is larger than that of stable DSs in saturated nonlinear media [18].

Finally, we take $\varepsilon = -0.2$ as a typical case of negative defect in order to study DSs. Also, we plot the DSs' power in Fig. 2a. In the contrast to the above both cases, when $\varepsilon = -0.2$, the stable DSs exist in the regions $5.86 \leq \mu \leq 7.44$ and $\mu \geq 8.1$, which correspond to in the first gap and the semi-infinite gap, respectively.

Figs. 3g–i show the evolution of the stable DS for $\mu = 6.5$ (point C in Fig. 2a) in the first gap. As shown in the Figs. 3g–i, the stable DS carrying lower power occupies more lattices besides the center lattice. However, In the region $7.90 \leq \mu < 8.10$, *i.e.*, near the edge of the band, the DSs are unstable, and the dependence of the soliton power on μ has a turning point, i.e., the soliton power does not increase with the growth of the propagation constant, as shown by the curve of power versus propagation constant in the inserted figure of the Fig. 2a. This result is similar to the defect solitons in the saturated nonlinear media [18]. The real part of the perturbation growth rate Re $(\lambda) > 0$ for unstable DSs is shown in Fig. 2b, and this result is in accordance with the VK criterion. Figs. 3j–3l are the profiles of DS for $\mu = 8$ (point D in Fig. 2a) at $z = 0$, $z = 20$ and $z = 40$, respectively. The unstable DS gradually spread into many lattice sites and decays eventually.
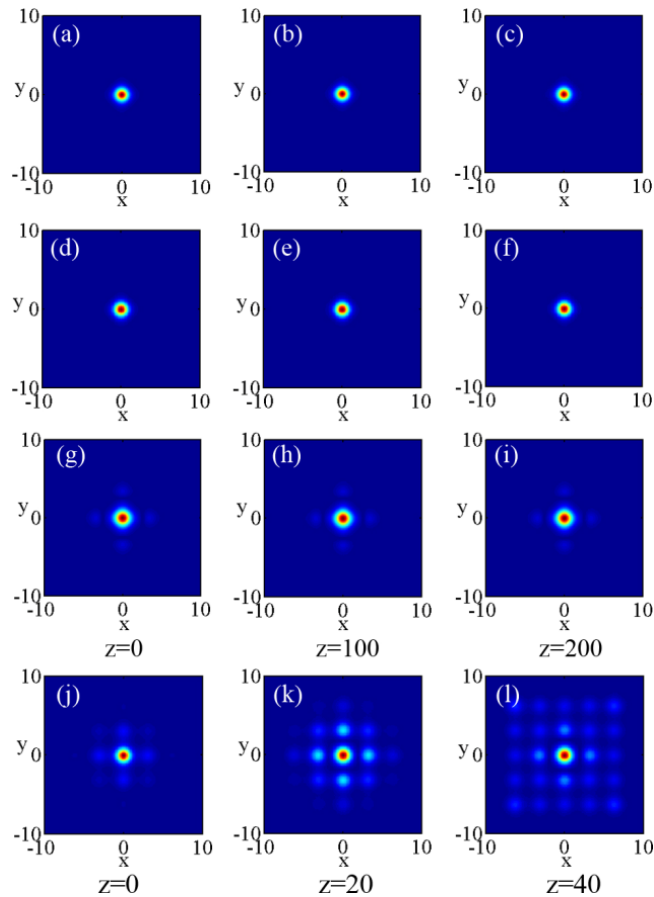

Fig. 3 (Color online) –a–c) Stable soliton for $\mu = 10$ (point A in Fig. 2a) when $\varepsilon = 0$; d–f) stable DS for $\mu = 11$ (point B in Fig. 2a) when $\varepsilon = 0.2$; g–i) stable DS for $\mu = 6.5$ (point C in Fig. 2a) when $\varepsilon = -0.2$; j–l) unstable DS for $\mu = 8$ (point D in Fig. 2a) when $\varepsilon = -0.2$.

3.2. THE DEFECT SOLITONS IN DEFOCUSING KERR MEDIA

In the case of defocusing Kerr media we have a different situation: the solitons in uniform lattices and in negative defect lattices both exist in the first gap, but not in the semi-infinite gap. The soliton power *P versus* the propagation constant μ is plotted in Fig. 4a. In addition, for the same propagation constant, the soliton powers in the case of positive defect is larger than those in uniform lattices and in the case of negative defect. These properties are in contrast to those corresponding to the focusing case as mentioned above.

For uniform lattices ($\varepsilon = 0$), solitons can exist in the first gap and all these solitons are stable. An example of stable soliton in uniform lattices is showed in Figs. 5a–5c corresponding to point A in Fig. 4a with $\mu = 6$.

For negative defect, the DSs only exist in the first gap with $\varepsilon > -0.3$. Here, we set $\varepsilon = -0.2$ to study the properties of DSs. When $\varepsilon = -0.2$, the DS exists in the region of $4.88 \leq \mu \leq 5.82$ locating at the first gap, and the DSs are all stable. We take $\mu = 5.5$ (point B in Fig. 4a) as an example to simulate the propagation of DS. Figs. 5d–5f are the profiles at $z = 0$, $z = 100$, and $z = 200$, respectively. Obviously, the DS is stable upon propagation.
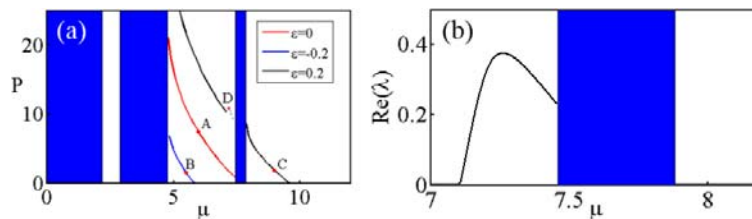

Fig. 4 (Color online) – a) The power of DSs *versus* propagation constant in defocusing media (blue shaded regions are Bloch bands – defocusing case); b) the real part of perturbation growth rate λ for the unstable DS when $\varepsilon = 0.2$.

For positive defect case, solitons exist in both the first gap and the semi-infinite gap. When $\varepsilon = 0.2$, the DS stably exists in the regions of $4.9 \leq \mu \leq 7.4$ (in the first gap) and $7.9 \leq \mu \leq 9.6$ (in the semi-infinite gap). Figs. 5g–5i show the evolution of a stable DS for $\mu = 9$ (point C in Fig. 4a). The DS can maintain its profile in propagation. But at the edge of the first gap, $7.13 \leq \mu \leq 7.41$, the solitons are unstable and accordingly, we see that one turning point of power versus propagation constant appears, which is similar to the focusing case where solitons exist at the edge of the semi-infinite gap (Fig. 2a). We also numerically calculate the real part of perturbation growth rate Re $\lambda > 0$ for the unstable region as shown in Fig. 4b; here the stability obeys the anti-VK criterion [22]. This can be explained as follows: the defocusing medium can defocus light and the defocusing capacity increases with the growth of the light intensity, *i.e.*, the light interaction with the nonlinear medium is contrary to the above focusing case. For the unstable case, we

take $\mu = 7.2$ (point D in Fig. 4a) to simulate soliton propagation, as displayed in Figs. 5j–5l. The unstable soliton gradually spreads into the nearby lattices and finally decays.
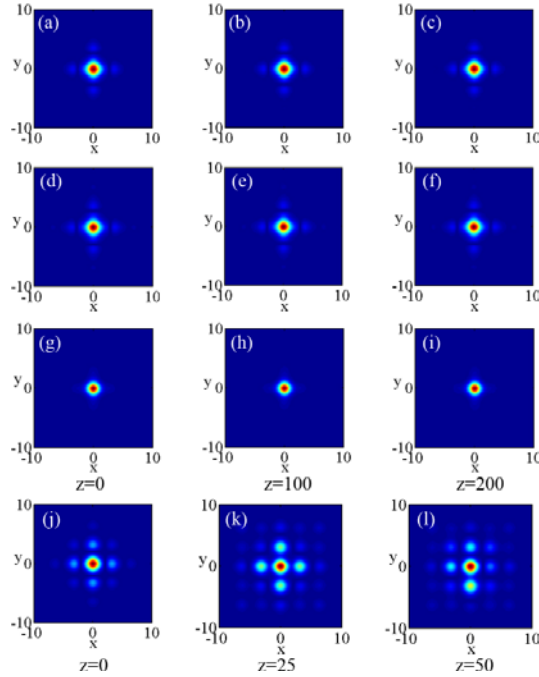

Fig. 5 (Color online) – a), b) and c) Stable soliton for $\mu = 6$ (point A in Fig. 4a) when $\varepsilon = 0$; d), e) and f) stable DS for $\mu = 5.5$ (point B in Fig. 4a) when $\varepsilon = -0.2$; g), h) and i) stable DS for $\mu = 9$ (point C in Fig. 4a) when $\varepsilon = 0.2$; j), k) and l) unstable DS for $\mu = 7.2$ (point D in Fig. 4a) when $\varepsilon = 0$.

4. CONCLUSIONS

We have studied the defect solitons in optical lattices based on both focusing and defocusing Kerr media. We revealed the stable regions of the defect solitons for different lattice defects in both the focusing and defocusing Kerr media. In focusing media, for negative defect, the defect solitons can exist in both the semi-infinite gap and in the first gap. In the semi-infinite gap, near the Bloch band, the defect solitons are unstable. In the first gap, defect solitons are stable. For the case of positive defect, solitons only exist in the semi-infinite gap and they are stable. In defocusing media, for the case of positive defect, such solitons can exist in both the first gap and the semi-infinite gap. In the first gap, at the edge of the Bloch band, defect solitons are unstable. In the semi-infinite gap, defect solitons are stable. For the case of the negative defect, such solitons only exist in the first gap, and they can be stable. Some of the results reported in this work are different from those

obtained in the case of saturable nonlinear media. Our results can be extended to higher-dimensional solitons, such as spatiotemporal optical solitons, alias "light bullets" [28–30].

REFERENCES

1. Y. V. Kartashov, V. A. Vysloukh, L. Torner, Progress in Optics, **52**, 63 (2009).
2. J. Yang, Z. Chen, Phys. Rev. E, **73**, 026609 (2006).
3. N. K. Efremidis, S. Sears, D. N. Christodoulides, Phys. Rev. E, **66**, 046602 (2002).
4. A. A. Sukhorukov, Y. S. Kivshar, Phys. Rev. Lett., **87**, 083901 (2001).
5. J. W. Fleischer, T. Carmon, M. Segev, Phys. Rev. Lett., **90**, 023902 (2003).
6. D. N. Neshev, T. J. Alexander, E. A. Ostrovskaya, Y. S. Kivshar, Phys. Rev. Lett., **92**, 123903 (2004).
7. J. W. Fleischer, M. Segev, N. K. Efremidis, D. N. Christodoulides, in Conference on *Lasers and Electro-Optics/Quantum Electronics and Laser Science Conference, Technical Digest*, Optical Society of America, 2003, paper QThK1.
8. M. Heinrich, Y. V. Kartashov, L. P. R. Ramirez, A. Szameit, F. Dreisow, R. Keil, S. Nolte, A. Tünnermann, V. A. Vysloukh, L. Torner, Opt. Lett., **34**, 3701 (2009).
9. J. K. Yang, Opt. Lett., **28**, 2094 (2003).
10. I. Makasyuk, Z. Chen, J. Yang, Phys. Rev. Lett., **96**, 223903 (2006).
11. V. Kuzmiak, A. A. Maradudin, F. Pincemin, Phys. Rev. B, **50**, 16835 (1994).
12. W. Chen, D. L. Mills, Phys. Rev. Lett., **58**, 160 (1987).
13. Y. V. Kartashov, V. A. Vysloukh, L. Torner, Phys. Rev. Lett., **96**, 073901 (2006).
14. D. N. Christodoulides, E. D. Eugenieva, Phys. Rev. Lett., **87**, 233901 (2001).
15. Y. V. Kartashov, B. A. Malomed, L. Torner, Rev. Mod. Phys., **83**, 247 (2011).
16. F. Fedele, J. Yang, Opt. Lett., **30**, 1506 (2005).
17. J. Wang, J. Yang, Phys. Rev. A, **76**, 013828 (2007).
18. W. Chen, X. Zhu, T. W. Wu, R. H. Li, Opt. Express, **18**, 10956 (2010).
19. X. Zhu, H. Wang, T. W. Wu, L. X. Zheng, J. Opt. Soc. Am. B, **28**, 521 (2011).
20. X. Zhu, H. Wang, L. Zheng, Opt. Express, **18**, 20786 (2010).
21. Y. Li, W. Pang, Y. Chen, Z. Yu, J. Zhou, H. Zhang, Phys. Rev. A, **80**, 043824 (2009).
22. H. Sakaguchi, B. A. Malomed. Phys. Rev. A, **81**, 013624 (2010).
23. N. K. Efremidis, J. Hudock, D. N. Christodoulides, J. W. Fleischer, O. Cohen, M. Segev, Phys. Rev. Lett., **91**, 213906 (3003).
24. J. Wang, J. Yang, Phys. Rev. A, **77**, 033834 (2008).
25. J. Yang, T. I. Lakoba, Stud. Appl. Math., **118**, 153 (2007).
26. V. Kuzmiak, A. A. Maradudin, F. Pincemin, Phys. Rev. B, **50**, 16835 (1994).
27. J. Yang, J. Comput. Phys., **227**, 6862 (2008).
28. D. Mihalache, J. Optoelectron. Adv. Mater., **12**, 12 (2010);
    D. Mihalache, Proc. Romanian Acad. A, **11**, 142 (2010);
    D. Mihalache, Rom. J. Phys., **57**, 352 (2012).
29. H. Leblond, B. A. Malomed, D. Mihalache, J. Optoelectron. Adv. Mater., **12**, 6 (2010).
30. D. Mihalache, J. Optoelectron. Adv. Mater., **13**, 1055 (2011);
    D. Mihalache, D. Mazilu, Rom. Rep. Phys., **60**, 749 (2008);
    D. Mihalache, Rom. Rep. Phys., **63**, 9 (2011).